International Journal of Engineering

Incorporated Poly Acrylic Acid-co-Fe$_3$O$_4$ Nanoparticles Mixed Matrix Polyethersulfone based Nanofiltration Membrane in Desalination Process

E. Bagheripour, A. R. Moghadassi*, S. M. Hosseini

Department of Chemical Engineering, Faculty of Engineering, Arak University, Arak, Iran

A B S T R A C T

Polyethersulfone (PES) based nanocomposite nanofiltration membrane was prepared by immersion precipitation method and casting solution technique using poly acrylic acid (PAA) grafted-iron oxide nanoparticles (Fe$_3$O$_4$) as hydrophilic filler additives. For this purpose, iron oxide nanoparticles were modified by in situ polymerization of acrylic acid in aqueous solution by potassium persulfate as initiator and ethylene glycol as cross-linker. The grafted iron oxide nanoparticles were investigated by Fourier transforms infrared spectroscopy. The effect of different concentrations of grafted nanoparticles on the PES nanofiltration membrane performance and properties was investigated by scanning electron microscopy, water content, pure water flux, pore size, permeability flux, rejection and tensile strength. The water content was enhanced by incorporation of nanoparticles into the membrane matrix from 72.04 to 74.75%. It was observed that pure water flux (2.68 to 8.71 L/m^2.h), mean pore size (2 to 6 nm) and permeability flux (0.8 to 4 L/m^2.h) improved with loading of nanoparticles into the membrane matrix. The results revealed that utilization of grafted iron oxide nanoparticles in the membrane matrix led to improvement of rejection from 53.98 to 89.19% for membrane filled with 0.05% wt. nanoparticles. Also tensile strength increased slightly for sample 1 from 3874 to 4825 kPa for sample 4. Moreover, results showed more appreciation performance for the modified membrane containing PAA-Fe$_3$O$_4$ composite nanofillers compared to membrane filled with bare Fe$_3$O$_4$ nanoparticles.

doi: 10.5829/ije.2017.30.06c.01

1. INTRODUCTION

In the recent years, membrane processes gradually have found their way to industrial applications and serve as alternatives for traditional processes such as desalination, evaporation and extraction. There are various membranes applicable for different separation processes depending on their physico-chemical specifications. Nanofiltration membrane is one type of membrane characterized by its surface charge and pore sizes [1]. Polyethersulfone (PES) has been extremely used as membrane fabrication material because of its appropriate properties. PES is a hydrophobic polymer and is easily susceptible to fouling. This results in severe restriction in permeate flux with constant

operation time [2]. Extensive efforts have been devoted to the improvement of PES membrane hydrophilicity and then antifouling property through a variety of methods such as surface grafting and additive blending [3-6]. Much attention has been especially paid in recent years to inorganic particles as membrane additives. These particles include Fe$_3$O$_4$, SiO$_2$, TiO$_2$ and Al$_2$O$_3$ and etc. The prepared membranes are expected to have a composite structure and combine the basic properties of polymers and inorganic particles [7-11]. Inserting inorganic nanoparticles in the membrane matrix can improve the strength and stiffness, hydrophilicity, water permeability and rejection and the antifouling properties of polymer based nanocomposite membranes [12-16].

Fe$_3$O$_4$ is one of the adsorptive inorganic particles used for preparation of membranes composed of inorganic- organic materials due to its good features such as excellent thermal and chemical stability,

Corresponding Author's Email: A.Moghadassi@Gmail.com (A. R. Moghadassi)

magnetic performance and good biodegradation and biocompatibility. These properties caused extensive use of this particle in various separation techniques such as preparing magnetic targeting medicine and magnetic fluids and preparing magnetic micro spheres for the quick separation of cellular, biomedical and bioengineering products [17].

Application of iron oxide as filler in polyvinyl alcohol nanocomposite pervaporation membrane was developed for dehydration of organic solvents [18]. Compared with other metal oxides, conspicuous impact of iron oxide nanoparticles on membranes performance for arsenic removal is reported [19, 20].

Since inorganic nanofillers typically are alien to organic matrices, the nanoparticles often agglomerate into clusters instead of dispersing uniformly in the polymer matrix. This can be avoided by using colloidal solutions of surface modified inorganic nanoparticles, subsequently transferring into a polymer matrix [21].

Generally, inorganic particles can be modified to form composite nanomaterials by chemical bonding or physical polymer adsorption on their surface. In the chemical bonding method, polymeric chains form on the inorganic particles surface by in situ polymerization (grafting processes) [22-26]. In this situation, particle–particle interaction between nanoparticles decreases leading to less agglomeration between them. Thus better dispersion is expected from them in membrane matrix [27]. However, these hybrid nanoparticles are expected as suitable additives for organic–inorganic composite membranes. Up to now, there is no report investigating the effect of PAA-g-Fe_3O_4 nanoparticles on the PES nano filtration (NF) membrane matrix performance and properties. However, combination of the nanoparticles and coating/grafting methods has been recently revealed that enhances the removal of organic and inorganic contaminants, elevates the mechanical strength, lowers the fouling, increases the flux recovery and adsorptive properties of membranes [28, 29].

This study was conducted to investigate the effect of PAA-g-Fe_3O_4 nanoparticles concentration on performance and properties of PES NF membrane. For this aim, prepared composite NF membranes were analyzed by scanning electron microscopy (SEM), pure water flux, permeability flux, rejection, water content, porosity, pore size and tensile strength. In addition, for ensuring grafting polymerization on Fe_3O_4 nanoparticles, the composite nanoparticles were analyzed by Fourier transform infrared spectroscopy (FTIR).

2. METHODS AND MATERIALS

2. 1. Materials   Polyethersulfone (PES) (Ultrason E6020P, MW= 58,000 g/mol, BASF) was used as the basic polymer. Polyvinylpyrrolidone (PVP) (MW= 25,000 g/mol, Merck) was used as a pore former. Fe_3O_4 nanoparticles (MW = 213.53 g/mol, APS = 60 nm, SSA > 55 m^2/g, purification= 99.2%, NANORADBEHAN Company, Iran) were used as inorganic nanoparticles. N, N-dimethylacetamide (DMAc) (Mw= 87.12 g/mol, Merck) and deionized water were used as solvent and non-solvent, respectively. All other chemicals were supplied by Merck.

2. 2. Modification of Fe_3O_4 Nanoparticles by PAA
Modification of Fe_3O_4 nanoparticles was performed by thermal in situ polymerization of AA in the aqueous solution using potassium persulfate (KPS) as an initiator in an air sealed glass container. Details of thermal in situ polymerization of AA in the aqueous solution were expressed in the published paper [21]. Briefly, 20 mg of Fe_3O_4 nanoparticles without any purification was added to 30 ml distilled water (DW) containing 2 g AA monomers, 400 mg ethylene glycol (EG) as cross linker and 10 mg KPS. The mixture was sonicated for 30 min for dispersion of Fe_3O_4 nanoparticles. Then, nitrogen gas was bubbled in aqueous solution for 15 min. The glass container was fixed in an oil bath on the heater-stirrer, heated to 90 ^{o}C and stirred vigorously at 400 rpm for 4 h. Finally, the product was washed repeatedly with DW and centrifuged (at 6000 rpm for 50 min) several times to remove any non-reacted AA monomers and unattached PAA. Finally, the prepared PAA/Fe_3O_4 nanocomposite particles were dried at 50 ^{o}C in an oven for 48 h.

2. 3. Fabrication of Mixed Matrix Nanocomposite PES/PAA-Fe_3O_4 Membrane   Flat sheet mixed matrix nanocomposite PES/PAA-Fe_3O_4 membranes were prepared by common immersion precipitation technique [12, 21]. Preparation proceeded by dissolving PES and PVP in solvent (DMAc) in glassy reactors equipped with mechanical stirrer (Model: Velp Scientifica Multi 6 stirrer) to observe homogeneous polymeric solutions. This was followed by dispersion of PAA-Fe_3O_4 nanocomposite particles with different concentrations as a modifier in the casting solutions. For better dispersion of particles and breaking up their aggregates, the solutions were sonicated 1 h using an ultrasonic instrument (Parsonic11Smodel, S/N PN-88159, Iran). Polymeric solutions were then cast onto the clean and dry glass plates at room temperature using a film applicator with constant thickness (150 μm). Then they were dipped immediately in deionized water baths (as non-solvent). The prepared membrane was kept in fresh deionized water for 24 h and then they were dried between two filter paper sheets at room temperature for one day before testing. The composition of different polymeric solutions is shown in Table 1.

TABLE 1. Composition of various casting solutions

Samples No.	PES (wt.%)	PVP (wt.%)	PAA-Fe$_3$O$_4$ nanofillers (wt.%)
1	20	1	0
2	20	1	0.05
3	20	1	0.1
4	20	1	0.5
5	20	1	1

2. 4. Characterization Methods

2. 4. 1. Confirmation of Grafted PAA onto the Fe$_3$O$_4$ Nanoparticles
Fourier transform infrared spectroscopy (FTIR) measurement was carried out to approve the grafting of PAA layer on the Fe$_3$O$_4$ nanoparticles surface. FTIR spectra analysis was done using the Galaxy series FTIR 5000 spectrometer. Scans were taken at 4 cm^{-1} resolution between 500 and 4000 cm^{-1}.

2. 4. 2. Membrane Water Content
Membrane water content is a factor for measuring the hydrophilicity of the membranes. The water content was measured as the weight difference between the dried membranes and swollen ones. The wet membrane was weighed initially (OHAUS, Pioneer™, readability: 10−4 gr, OHAUS Corp., USA) and then was dried in an oven (Behdad Co., Model: O5, Iran) at a fixed temperature (50 $^{\circ}$C) for 24 h. The bellow equation was employed to determine the water conten [30]:

$$Water\ content\% = (\frac{W_w - W_d}{W_w}) \times 100 \tag{1}$$

where W_w and W_d are the wet and dry membrane weights (g), respectively. For minimizing the experimental errors, all measurements were performed three times for each membrane and their average values were reported.

2. 4. 3. Pore size measurement
In order to determine the membrane mean pore radius size (rm), Guerout–Elford–Ferry equation basically on the pure water flux data was used [31].

$$r_m = \sqrt{\frac{(2.9 - 1.75 Porosity) 8\eta l Q}{Porosity * A * \Delta P}} \tag{2}$$

here η is the water viscosity (8.9   Pa.s), l is the membrane thickness (m), Q is pure water permeated (m^3/s), and ΔP is the operating pressure (6 bar).

2. 4. 4. Scanning Electron Microscopy (SEM)
In order to study the morphology, structure and pore shape of the prepared membranes, scanning electron microscopes (SEM) (Seron Technology Inc. Korea) was employed. The membranes were cut to small pieces and submerged in nitrogen liquid for 5 min. The frozen membranes were broken and kept in air for drying. The dried membranes were gold sputtered to provide electrical conductivity. Photomicrographs were taken under very high vacuum condition at 15 kV.

2. 4. 5. Membrane Performance
NF experiments were carried out with a process in dead end cell. The mentioned experimental setup is shown schematically in Figure 1. Nitrogen gas was used as the cell driving force. Membrane samples were cut in the cell size and placed into the cell by top surface contacting feed solution. Operation pressure was fixed at 6 bar for all experiments. Aqueous sodium sulfate solution (1000 mg/l) was used as feed. The permeability flux was calculated as follows [30]:

$$J_v = (\frac{V}{A * \Delta t}) \tag{3}$$

where Jv, V, A and Δt are permeability flux (L/m^{2}h), quantity of permeate (L), membrane area (m^2) and filtration time (h), respectively.

Moreover, salt removal efficiency was calculated using bellow equation [32, 33]:

$$Re\ jection\ \% = (\frac{C_f - C_p}{C_f}) * 100 \tag{4}$$

where C_p and C_f reflect the sodium sulfate concentrations in permeate and feed solutions, respectively, both measured by conductivity meter (Ohaus Corporation, S/N B143385306, U.S.A).

2. 4. 6. Mechanical Properties
For describing the mechanical properties changes as a result of PAA-Fe$_3$O$_4$ nanoparticles addition in the casting solution, membrane's tensile strength at break point is an appropriate benchmark. For this aim, their mechanical characterization was measured according to ASTM1922-03 [34]. Samples were cut in the standard shapes and the experiments were done triple to minimize the experimental errors.
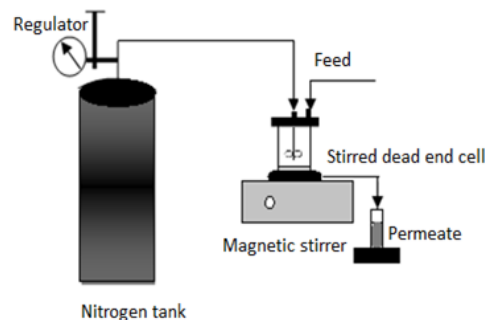

Figure 1. Schematic diagram of dead end cell experimental set up

3. RESULTS AND DISCUSSION

3. 1. Confirmation of PAA Grafted on Fe_3O_4
FTIR analysis of bare Fe_3O_4 nanoparticles and PAA-g-Fe_3O_4 nanofillers is shown in Figure 2. Results show appearing the peaks related to C=O and CH_2 at 1766 and 3100 cm^{-1} which decisively prove the graft polymerization of PAA on Fe_3O_4 nanoparticles. This is not visible for bare Fe_3O_4 nanoparticles.

3. 2. Hydrophilicity
The affinity of a membrane to get wet is defined as water content which is a scale of membrane hydrophilicity [35, 36]. The effect of PAA-Fe_3O_4 nanocomposite fillers concentration on the membrane water content is shown in Figure 3. Results (Figure 3) showed that membrane water content generally increased by addition of nanofillers with various concentrations. This can be due to the hydrophilic characteristic of PAA-Fe_3O_4 nanocomposite fillers. Moreover it can be due to increase of pore size and number in the presence of PAA-Fe_3O_4 nanocomposite particles [36], leading to more space for water adsorption and saving. The highest water content was obtained for sample 2 containing 0.05 wt.% nanofillers. It means that this membrane has the most hydrophilicity compared to others. As it is clear, a reduction in water content was be seen for sample 3 which contains 0.1 wt.% nanocomposite particles. This may be due to the voids and cavities filling by PAA-Fe_3O_4 nanocomposite fillers which can be prevailed upon the positive effect of nanofillers hydrophilic characteristic [21, 29] which results in reduction of membrane porosity and so restricts the water molecules accommodation in the membrane structure leading to decrease in water adsorption and water content.
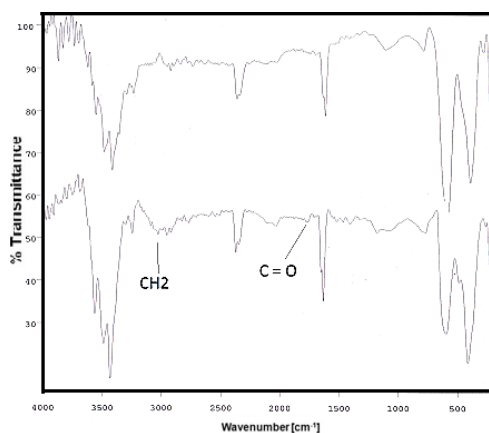

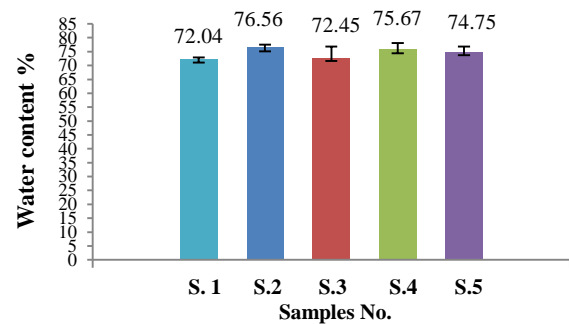**Figure 3.** The effect of PAA-Fe_3O_4 nanocomposite particles concentration on water content

3. 3. Morphological Study
SEM images were taken to evaluate the changes in morphology made by various contents of PAA-Fe_3O_4 nanocomposite fillers in the casting solution. Cross-sectional SEM images are presented in Figure 4. As can be seen, all the membranes show typical characteristic of asymmetric porous structure with finger-like sub-layer and dense top-layer. These images clearly show changes formed in membranes pore and channels shape due to PAA-Fe_3O_4 nanocomposite fillers addition in the casting solution. SEM images (Figure 4) revealed that pores and channels radius at top and sub-layer increase by increasing nanofiller concentration to 0.5 wt.% and then decreased in 1 wt.% nanofillers loading rate. Higher affinity between polymeric solution containing hydrophilic PAA-Fe_3O_4 nanocomposite fillers and water (non-solvent) in comparison to bare PES, promotes exchanging of solvent and non-solvent during phase inversion process, leading to formation of membrane with wider voids and channels in the membrane matrix (SEM images Figures 4b, c and d). But increasing the viscosity of casting solution by increasing nanofillers loading ratio to 1wt. % decreases the coagulation rate of the polymer in non-solvent during phase inversion process and offers lower porosity in membrane structure (SEM image f).

3. 4. Membranes Performance
Figure 5 demonstrates the pure water flux of the prepared PES membrane with and without nanofillers. As can be seen, pure water flux at PAA-Fe_3O_4 nanocomposite fillers loading range of 0-0.5 wt.% initially increased from 2.68 to 8.71 L/m^2.h and then decreased to 6.03 L/m^2.h for sample 5 (1wt.% nanofiller). Porosity and hydrophilicity are two main factors affecting water flux [37]. As seen before in SEM images (Figure 4), more porosity was observed in samples 2, 3 and 4. Additionally, water content results generally introduced higher hydrophilicity to membranes filled with nanofillers.
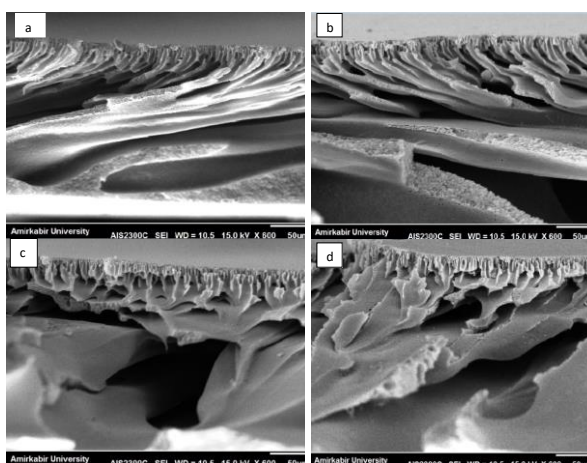

Figure 2. FTIR spectra of Fe_3O_4 and PAA/Fe_3O_4 nanoparticles

Figure 4. The SEM images of cross-section of fabricated membranes with different concentrations of PAA-Fe$_3$O$_4$ nanocomposite particles: (a) Sample 1, (b) Sample 2, (c) Sample 3, (d) Sample 4 and (f) Sample 5

Therefore, higher porosity and hydrophilicity can make it easy for water passing through the membrane leading to improvement of pure water flux.

A similar trend is also observed for mean pore size calculated by Equation (2) (Figure 6). Also some published researches reported same results [37, 38].

As seen in Figure 4, due to increase of casting solution viscosity at high nanofiller content (1wt.%), lower porosity was observed for sample 5. Thus, it can be concluded that declined pure water flux in this nanofiller loading rate, partly may be related to reduction of porosity caused by increasing the casting solution viscosity (see Figure 4, image f).

Also Figure 7 shows a cross-sectional SEM image of sample 5 (filled with 1 wt.% nanofillers) by 4k magnification. As can be seen in this Figure, very obvious pore blockage/filling and nanofillers agglomeration were observed at this nanofiller loading rate. This image confirms reduction of pore size and channels capability for passage of water molecules across the membrane. The results presented in Figure 6 (pore size) also covers both pore blockage/filling issue and porosity reduction at high nanofiller loading rate (1wt.%). Thus, pore size reduction caused by excessive nanofillers and agglomerated ones can be another reason for decline of pure water flux for sample 5.

The effect of PAA-Fe$_3$O$_4$ nanocomposite fillers concentration on permeability and salt rejection is shown in Figure 8. The obtained results showed that permeability flux improved from 0.8 for bare PES to about 4 (L/m^2.h) for the membrane containing 0.5 wt.% nanofillers. This behavior can be explained by water content improvement (Figure 3), porosity increment (Figure 4, SEM images b, c and d) and growth in pores size (Figure 6) caused by PAA-Fe$_3$O$_4$ nanocomposite

fillers which are in a great agreement with permeability flux. According to Figure 8, permeability flux decreased for sample 5 (containing 1wt.% nanofiller). As mentioned before, water content decreased for sample 5 compared to sample 4 (containing 0.5 wt.% particles) and more compact structure was observed for sample 5 in Figure 4. Also a reduction of pore size was observed in Figure 6 for sample 5. It seems that like pure water flux, reduction of hydrophilicity (more hydrophobic membrane), restricted porosity and pore size are as main reasons for a drop in permeability flux at 1 wt.% nanofiller loading rate. Obtained results (Figure 8) revealed that by increase of PAA-Fe$_3$O$_4$ nanocomposite fillers content in the casting solution, the prepared membranes show two different behaviors against salt rejection. Increase of nanofiller content from 0 (bare PES) to 0.05 wt.% (sample2) strongly improved the sodium sulfate rejection from 54 to 89%. This can be explained by structural and morphological changes of the membrane during modification by PAA-Fe$_3$O$_4$ nanocomposite fillers. It is worth mentioning that for the applications of membranes in aqueous solution, hydrophilic membrane surface causes lower adsorption of macromolecular solutes or particles on the membrane surface and leading to rejection improvement [39, 40]. It seems that increasing of membrane hydrophilicity for sample 2 (see Figure 3), be as the main reason for enhancement of rejection in this nanofiller loading range. As can be seen in Figure 8, presence of higher contents of nanofillers in the casting solution caused continuing reduction of salt rejection from 89 to about 64%. The reduction in this nanofiller loading range may be related to more open structure, more porosity and growth of membrane pores size as seen in Figure 4 (SEM images c and d) and Figure 6, respectively. It is very well known that while the membrane structure turns to more open structure with higher porosity (in both top and sub-layer), it tends to result in higher permeate flux with lower separation performance [36].

Additionally, the reduction of rejection for sample 5 may be due to agglomeration of PAA-Fe$_3$O$_4$ nanocomposite fillers at high loading range (1wt.%) as it was seen in Figure 7. At this condition, the nanofillers active surface area reduces, leading to lower hydrophilic sites for water adsorption (see Figure 3) and weak wetting of the pores phenomenon. Therefore, adsorption and percipitation of ions and solutes on the membrane surface increases the rejection in this nanofiller loading range [2, 40].

3. 5. The Effect of PAA-Fe$_3$O$_4$ Nanocomposite Fillers on Mechanical Properties   The effect of PAA-Fe$_3$O$_4$ nanocomposite fillers on tensile strength is shown in Figure 9. Results indicated two various behaviors for membrane filled by PAA-Fe$_3$O$_4$ nanocomposite fillers against breaking force.
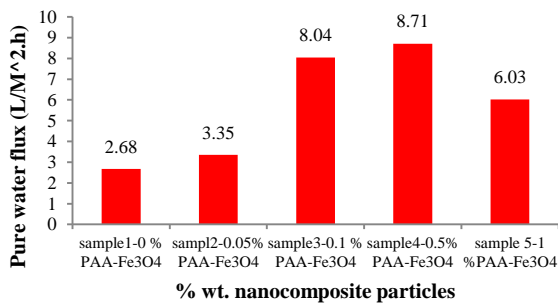
Figure 5. The effect of PAA-Fe$_3$O$_4$ nanocomposite particles concentration on pure water flux
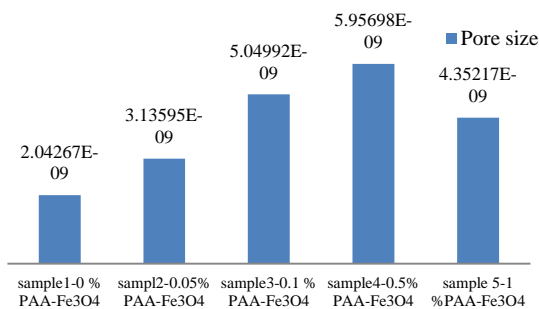

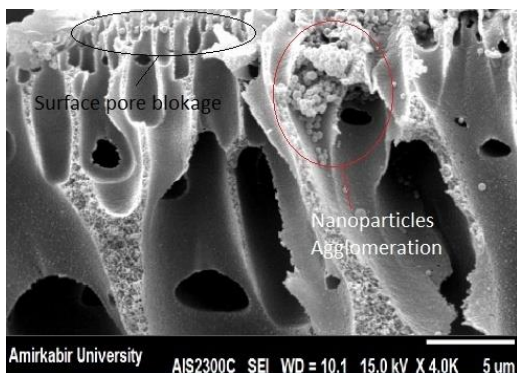**Figure 6.** The effect of PAA-Fe$_3$O$_4$ nanocomposite particles concentration on mean pore size (m)

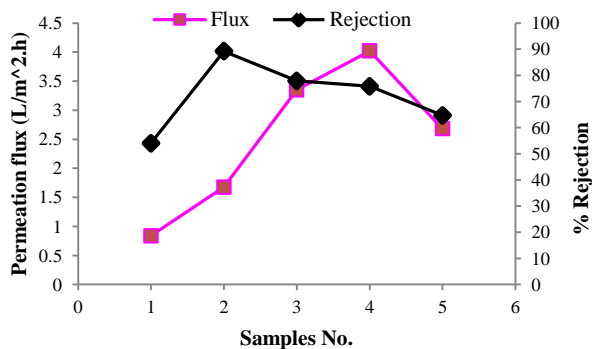**Figure 7.** Surface pore blockage and nanocomposite particles agglomeration in 1 wt.% PAA-Fe$_3$O$_4$ particles

Figure 8. The effect of PAA-Fe$_3$O$_4$ nanocomposite particles concentration on membrane performance

Membrane tensile strength increased initially from 3874 kPa (for bare PES) to 4825 kPa (membrane filled with 0.5wt.% nanofillers) and then decreased to 3866 kPa by 1wt.% nanofillers loading rate. In fact, it can be concluded that the PAA-Fe$_3$O$_4$ nanocomposite fillers with appropriate concentration and dispersion play reinforced role in membrane matrix. It reinforces membranes at nanofiller loading range of 0-0.5wt.% by formation of strong interfacial bonding between polymers and additive, leading to more membrane rigidity [41]. Results (Figure 9) revealed that tensile strength decreased for sample 5 filled by 1wt.% nanofillers. As inferred from the results of Figure 8, excessive amounts of PAA-Fe$_3$O$_4$ nanocomposite fillers tend to form agglomeration and discrete phase in the membrane. At this condition, nanofillers distribute non-uniformly in the prepared membranes and lead to reduction in the membrane endurance for load stress.

3 .6. Comparison between Bare Fe$_3$O$_4$ and PAA-Fe$_3$O$_4$ Nanocomposite Fillers on PES Performance
In order to compare the effect of Fe$_3$O$_4$ and PAA-Fe$_3$O$_4$ nanocomposite fillers on PES performance, one more nanocomposite membrane was prepared similar to sample 5, just instead of PAA-Fe$_3$O$_4$ nanofiller, bare Fe$_3$O$_4$ nanoparticles were incorporated into the casting solution. The comparison results are shown in Figure 10. The obtained results (Figure 10) revealed that both permeability flux and salt rejection of membrane filled by PAA-Fe$_3$O$_4$ nanocomposite fillers are higher than that of Fe$_3$O$_4$ nanoparticles. This can be due to a better dispersion of PAA-Fe$_3$O$_4$ nanofillers compared to bare Fe$_3$O$_4$. In the other word, it can be said that presence of a thin layer of PAA formed on the Fe$_3$O$_4$ nanoparticles surface, decreases the Fe$_3$O$_4$ nanoparticles interaction and may cause better dispersion of it in the membrane matrix. Thus its capability to influence on membrane performance becomes more. In addition, presence of hydrophilic PAA on Fe$_3$O$_4$ nanoparticles surface and enhancement of its hydrophilicity can be as another reason for better performance of PAA-Fe$_3$O$_4$ compared to Fe$_3$O$_4$.
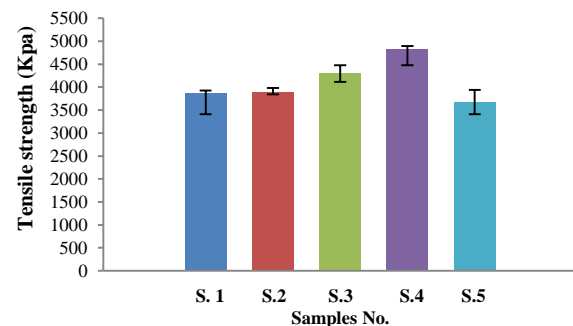

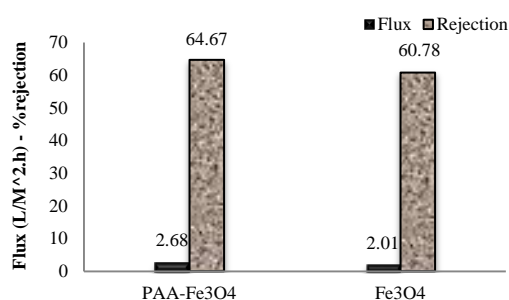**Figure 9.** The effect of iron-nickel oxide nanoparticle concentration on tensile strength

Figure 10. Comparison between Fe_3O_4 and PAA-Fe_3O_4 effect on membrane performance

4. CONCLUSION

A novel PES/PAA-Fe_3O_4 nanofiltration membrane was prepared and characterized. For this purpose, firstly PAA-Fe_3O_4 nanocomposite particles were provided using poly (acrylic acid) grafted on iron oxide (Fe_3O_4) nanoparticles. FTIR spectra analysis obviously proved the graft polymerization of PAA-Fe_3O_4. It was found that membrane water content generally increased by addition of PAA-Fe_3O_4 nanocomposite fillers with various concentrations. SEM images showed that porosity in sub-layer increased initially by addition of PAA-Fe_3O_4 nanocomposite fillers and decreased again using 1 wt% nanofillers in the casting solution. The obtained results revealed that membrane pure water flux, mean pore size and permeation flux have a straight relation together and they were improved initially by increasing of nanofillers content at 0-0.5wt.% loading range and again deducted by application of higher amount of nanofillers in the casting solution. Moreover, salt rejection enhanced by addition of 0.05 wt.% PAA-Fe_3O_4 nanocomposite fillers and then decreased. The measured tensile strength results revealed an improvement due to PAA-Fe_3O_4 presence in the membrane structure in all samples except at 1wt.% nanofillers loading rate. Additionally, for comparison between Fe_3O_4 and PAA-Fe_3O_4, their effect on the permeability and rejection was studied separately. The results indicated better performance of PAA-Fe_3O_4 at both permeability and rejection compared to Fe_3O_4. Regarding the obtained results and performance of prepared membranes, the optimum concentration of PAA-Fe_3O_4 nanoparticles was found to be 0.5 wt.% with the highest flux and a reasonable rejection.

5. ACKNOWLEDGMENT

6. REFERENCES

1. Bagheripour, E., Moghadassi, A. and Hosseini, S., "Preparation of polyvinylchloride nanofiltration membrane: Investigation of the effect of thickness, prior evaporation time and addition of polyethylenglchol as additive on membrane performance and properties", *International Journal of Engineering-Transactions C: Aspects*, Vol. 29, No. 3, (2016), 280.

2. Luo, M.-L., Zhao, J.-Q., Tang, W. and Pu, C.-S., "Hydrophilic modification of poly (ether sulfone) ultrafiltration membrane surface by self-assembly of TiO_2 nanoparticles", *Applied Surface Science*, Vol. 249, No. 1, (2005), 76-84.

3. Ulbricht, M. and Belfort, G., "Surface modification of ultrafiltration membranes by low temperature plasma ii. Graft polymerization onto polyacrylonitrile and polysulfone", *Journal of Membrane Science*, Vol. 111, No. 2, (1996), 193-215.

4. Che, A.-F., Huang, X.-J. and Xu, Z.-K., "Polyacrylonitrile-based nanofibrous membrane with glycosylated surface for lectin affinity adsorption", *Journal of Membrane Science*, Vol. 366, No. 1, (2011), 272-277.

5. Ulbricht, M., Matuschewski, H., Oechel, A. and Hicke, H.-G., "Photo-induced graft polymerization surface modifications for the preparation of hydrophilic and low-proten-adsorbing ultrafiltration membranes", *Journal of Membrane Science*, Vol. 115, No. 1, (1996), 31-47.

6. Fei, Z.-D., Wan, L.-S., Wang, W.-M., Zhong, M.-Q. and Xu, Z.-K., "Thermo-responsive polyacrylonitrile membranes prepared with poly (acrylonitrile-g-isopropylacrylamide) as an additive", *Journal of Membrane Science*, Vol. 432, (2013), 42-49.

7. Huang, Z.-Q., Chen, Z.-Y., Guo, X.-P., Zhang, Z. and Guo, C.-L., "Structures and separation properties of pan− fe3o4 ultrafiltration membranes prepared under an orthogonal magnetic field", *Industrial & engineering chemistry research*, Vol. 45, No. 23, (2006), 7905-7912.

8. Khan, A.A. and Baig, U., "Polyacrylonitrile-based organic-inorganic composite anion-exchange membranes: Preparation, characterization and its application in making ion-selective membrane electrode for determination of as (v)", *Desalination*, Vol. 289, (2012), 21-26.

9. Jung, H.-R., Ju, D.-H., Lee, W.-J., Zhang, X. and Kotek, R., "Electrospun hydrophilic fumed silica/polyacrylonitrile nanofiber-based composite electrolyte membranes", *Electrochimica Acta*, Vol. 54, No. 13, (2009), 3630-3637.

10. Zhang, G., Zhang, J., Wang, L., Meng, Q. and Wang, J., "Fouling mechanism of low-pressure hollow fiber membranes used in separating nanosized photocatalysts", *Journal of Membrane Science*, Vol. 389, (2012), 532-543.

11. Maximous, N., Nakhla, G., Wan, W. and Wong, K., "Preparation, characterization and performance of Al_2O_3/pes membrane for wastewater filtration", *Journal of Membrane Science*, Vol. 341, No. 1, (2009), 67-75.

12. Vatanpour, V., Madaeni, S.S., Moradian, R., Zinadini, S. and Astinchap, B., "Novel antibifouling nanofiltration polyethersulfone membrane fabricated from embedding tio 2 coated multiwalled carbon nanotubes", *Separation and Purification Technology*, Vol. 90, (2012), 69-82.

13. Soroko, I., Lopes, M.P. and Livingston, A., "The effect of membrane formation parameters on performance of polyimide membranes for organic solvent nanofiltration (OSN): Part a. Effect of polymer/solvent/non-solvent system choice", *Journal of Membrane Science*, Vol. 381, No. 1, (2011), 152-162.

14. Soroko, I., Makowski, M., Spill, F. and Livingston, A., "The effect of membrane formation parameters on performance of polyimide membranes for organic solvent nanofiltration (OSN). Part b: Analysis of evaporation step and the role of a co-

solvent", *Journal of Membrane Science*,   Vol. 381, No. 1, (2011), 163-171.

15. Wei, X.-Z., Zhu, L.-P., Deng, H.-Y., Xu, Y.-Y., Zhu, B.-K. and Huang, Z.-M., "New type of nanofiltration membrane based on crosslinked hyperbranched polymers", *Journal of Membrane Science*, Vol. 323, No. 2, (2008), 278-287.

16. Badruddoza, A., Tay, A., Tan, P., Hidajat, K. and Uddin, M., "Carboxymethyl-β-cyclodextrin conjugated magnetic nanoparticles as nano-adsorbents for removal of copper ions: Synthesis and adsorption studies", *Journal of Hazardous Materials*, Vol. 185, No. 2, (2011), 1177-1186.

17. Madaeni, S., Zinadini, S. and Vatanpour, V., "Convective flow adsorption of nickel ions in pvdf membrane embedded with multi-walled carbon nanotubes and paa coating", *Separation and Purification Technology*, Vol. 80, No. 1, (2011), 155-162.

18. Sairam, M., Naidu, B.V.K., Nataraj, S.K., Sreedhar, B. and Aminabhavi, T.M., "Poly (vinyl alcohol)-iron oxide nanocomposite membranes for pervaporation dehydration of isopropanol, 1, 4-dioxane and tetrahydrofuran", *Journal of Membrane Science*, Vol. 283, No. 1, (2006), 65-73.

19. Sabbatini, P., Yrazu, F., Rossi, F., Thern, G., Marajofsky, A. and de Cortalezzi, M.F., "Fabrication and characterization of iron oxide ceramic membranes for arsenic removal", *Water Research*, Vol. 44, No. 19, (2010), 5702-5712.

20. Park, H. and Choi, H., "As (iii) removal by hybrid reactive membrane process combined with ozonation", *Water Research*, Vol. 45, No. 5, (2011), 1933-1940.

21. Daraei, P., Madaeni, S.S., Ghaemi, N., Monfared, H.A. and Khadivi, M.A., "Fabrication of pes nanofiltration membrane by simultaneous use of multi-walled carbon nanotube and surface graft polymerization method: Comparison of mwcnt and paa modified mwcnt", *Separation and Purification Technology*, Vol. 104, No., (2013), 32-44.

22. Taniguchi, T., Kashiwakura, T., Inada, T., Kunisada, Y., Kasuya, M., Kohri, M. and Nakahira, T., "Preparation of organic/inorganic composites by deposition of silica onto shell layers of polystyrene (core)/poly [2-(n, n-dimethylamino) ethyl methacrylate](shell) particles", *Journal of Colloid and Interface Science*, Vol. 347, No. 1, (2010), 62-68.

23. Gao, B., Chen, Y. and Zhang, Z., "Preparation of functional composite grafted particles pdmaema/sio 2 and preliminarily study on functionality", *Applied Surface Science*, Vol. 257, No. 1, (2010), 254-260.

24. Li, Y. and Benicewicz, B.C., "Functionalization of silica nanoparticles via the combination of surface-initiated raft polymerization and click reactions", *Macromolecules*, Vol. 41, No. 21, (2008), 7986-7992.

25. Huang, Y., Liu, Q., Zhou, X., Perrier, S.b. and Zhao, Y., "Synthesis of silica particles grafted with well-defined living polymeric chains by combination of raft polymerization and coupling reaction", *Macromolecules*, Vol. 42, No. 15, (2009), 5509-5517.

26. You, Y.-Z., Kalebaila, K.K., Brock, S.L. and Oupicky, D., "Temperature-controlled uptake and release in pnipam-modified porous silica nanoparticles", *Chemistry of Materials*, Vol. 20, No. 10, (2008), 3354-3359.

27. Zhi, S.-H., Deng, R., Xu, J., Wan, L.-S. and Xu, Z.-K., "Composite membranes from polyacrylonitrile with poly (n, n-dimethylaminoethyl methacrylate)-grafted silica nanoparticles as additives", *Reactive and Functional Polymers*, Vol. 86, (2015), 184-190.

28. Roy, S., Ntim, S.A., Mitra, S. and Sirkar, K.K., "Facile fabrication of superior nanofiltration membranes from interfacially polymerized cnt-polymer composites", *Journal of Membrane Science*, Vol. 375, No. 1, (2011), 81-87.

29. Madaeni, S., Zinadini, S. and Vatanpour, V., "A new approach to improve antifouling property of pvdf membrane using in situ polymerization of paa functionalized TiO_2 nanoparticles", *Journal of Membrane Science*, Vol. 380, No. 1, (2011), 155-162.

30. Han, R., Zhang, S., Liu, C., Wang, Y. and Jian, X., "Effect of naa zeolite performance", *Journal of Membrane Science*, Vol. 345, (2009), 5-12.

31. Hamid, N., Ismail, A.F., Matsuura, T., Zularisam, A., Lau, W.J., Yuliwati, E. and Abdullah, M.S., "Morphological and separation performance study of polysulfone/titanium dioxide (PSF/ TiO_2) ultrafiltration membranes for humic acid removal", *Desalination*, Vol. 273, No. 1, (2011), 85-92.

32. Lee, H.S., Im, S.J., Kim, J.H., Kim, H.J., Kim, J.P. and Min, B.R., "Polyamide thin-film nanofiltration membranes containing tio2 nanoparticles", *Desalination*, Vol. 219, No. 1-3, (2008), 48-56.

33. Hegde, C., Isloor, A.M., Padaki, M. and Fun, H.-K., "Synthesis and performance characterization of ps-ppees nanoporous membranes with nonwoven porous support", *Arabian Journal of Chemistry*, Vol. 6, No. 3, (2013), 319-326.

34. Gholami, A., Moghadassi, A., Hosseini, S., Shabani, S. and Gholami, F., "Preparation and characterization of polyvinyl chloride based nanocomposite nanofiltration-membrane modified by iron oxide nanoparticles for lead removal from water", *Journal of Industrial and Engineering Chemistry*, Vol. 20, No. 4, (2014), 1517-1522.

35. Sivakumar, M., Mohan, D.R. and Rangarajan, R., "Studies on cellulose acetate-polysulfone ultrafiltration membranes: Ii. Effect of additive concentration", *Journal of Membrane Science*, Vol. 268, No. 2, (2006), 208-219.

36. Mobarakabad, P., Moghadassi, A. and Hosseini, S., "Fabrication and characterization of poly (phenylene ether-ether sulfone) based nanofiltration membranes modified by titanium dioxide nanoparticles for water desalination", *Desalination*, Vol. 365, (2015), 227-233.

37. Zinadini, S., Zinatizadeh, A.A., Rahimi, M., Vatanpour, V. and Zangeneh, H., "Preparation of a novel antifouling mixed matrix pes membrane by embedding graphene oxide nanoplates", *Journal of Membrane Science*, Vol. 453, (2014), 292-301.

38. Safarpour, M., Khataee, A. and Vatanpour, V., "Effect of reduced graphene oxide/ TiO_2 nanocomposite with different molar ratios on the performance of pvdf ultrafiltration membranes", *Separation and Purification Technology*, Vol. 140, (2015), 32-42.

39. Machado, P., Habert, A. and Borges, C., "Membrane formation mechanism based on precipitation kinetics and membrane morphology: Flat and hollow fiber polysulfone membranes", *Journal of Membrane Science*, Vol. 155, No. 2, (1999), 171-183.

40. Borneman, Z., Zhang, W., Van den Boomgaard, T. and Smolders, C., "Semi-continuous protein fractionating using affinity cross-flow filtration", *Desalination*, Vol. 144, No. 1-3, (2002), 295-299.

41. Wu, G., Gan, S., Cui, L. and Xu, Y., "Preparation and characterization of pes/tio 2 composite membranes", *Applied Surface Science*, Vol. 254, No. 21, (2008), 7080-7086.

Incorporated Poly Acrylic Acid-co-Fe$_3$O$_4$ Nanoparticles Mixed Matrix Polyethersulfone based Nanofiltration Membrane in Desalination Process

E. Bagheripour, A. R. Moghadassi, S. M. Hosseini

Department of Chemical Engineering, Faculty of Engineering, Arak University, Arak, Iran

چکیده

غشای نانوکامپوزیت نانوفیلتراسیون بر پایه پلی اترسولفون با تکنیک محلول پلیمری و غوطه وری با استفاده از پرکننده نانوذرات اکسید آهن لایه نشانی شده با پلی آکریلیک اسید به عنوان افزودنی آبدوست ساخته شد. برای این منظور، نانوذرات اکسید آهن با استفاده از پلیمریزاسیون سطحی آکریلیک اسید در محلول آبی حاوی پتاسیم پرسولفات به عنوان شروع کننده واکنش و اتیلن گلایکول به عنوان اتصال دهنده عرضی اصلاح شدند. نانوذرات اکسید آهن پوشش داده شده با طیف سنجی مادون قرمز مورد ارزیابی قرار گرفتند. اثر افزودن غلظت های مختلف از این نانوذرات بر خواص و عملکرد غشای نانوفیلتراسیون پلی اتر سولفون با استفاده از میکروسکوپ الکترونی، میزان محتوی آب، شار آب خالص، اندازه حفرات، شار عبوری، جداسازی و مقاومت مکانیکی مورد بررسی قرار گرفت. محتوای آب با افزودن نانوذرات در ساختار غشا از مقدار ۷۲/۰۴ درصد تا ۷۴/۷۵ درصد بهبود یافت. مقدار شار آب خالص از مقدار ۲/۶۸ تا ۸/۷۱ لیتر بر واحد سطح و زمان، افزایش یافت. اندازه حفرات از مقدار ۲ نانو متر تا ۶ نانو متر و شار آب عبوری از ۰/۸ تا ۴ اضافه شدند. نتایج نشان داد استفاده از نانوذرات اکسید آهن پوشش داده شده با آکریلیک اسید در ساختار غشا باعث افزایش جداسازی از ۵۳/۹۸ درصد تا ۸۹/۱۹ درصد برای غشای دارای ۰/۰۵ درصد از نانوذرات شد. مقاومت مکانیکی به طور مستقیم از مقدار ۳۸۷۴ تا ۴۸۲۵ کیلوپاسکال افزایش یافت. به علاوه نتایج شار و درصد جداسازی بهتری برای غشای پر شده با نانوذرات پوشش داده شده نسبت به نانوذرات خالص مشاهده شد.

doi: *10.5829/ije.2017.30.06c.01*